Electromigration and potentiometry measurements of single-crystalline Ag nanowires under UHV conditions

2009 J. Phys.: Condens. Matter 21 265601

(http://iopscience.iop.org/0953-8984/21/26/265601)

J. Phys.: Condens. Matter **21** (2009) 265601 (6pp) doi:10.1088/0953-8984/21/26/265601

Electromigration and potentiometry measurements of single-crystalline Ag nanowires under UHV conditions

M R Kaspers[1], A M Bernhart[1], F-J Meyer zu Heringdorf[1,2], G Dumpich[1] and R Möller[1,2]

[1] Department of Physics, University of Duisburg-Essen, Lotharstrasse 1, 47048 Duisburg, Germany
[2] Center for Nanointegration Duisburg-Essen (CeNIDE), 47048 Duisburg, Germany

E-mail: mark.kaspers@uni-due.de

Received 19 February 2009, in final form 29 April 2009
Published 5 June 2009
Online at stacks.iop.org/JPhysCM/21/265601

Abstract

We report on *in situ* electromigration and potentiometry measurements on single-crystalline Ag nanowires under ultra-high vacuum (UHV) conditions, using a four-probe scanning tunnelling microscope (STM). The Ag nanowires are grown in place by self-organization on a 4° vicinal Si(001) surface. Two of the four available STM tips are used to contact the nanowire. The positioning of the tips is controlled by a scanning electron microscope (SEM). Potentiometry measurements on an Ag nanowire were carried out using a third tip to determine the resistance per length. During electromigration measurements current densities of up to 1×10^8 A cm^{-2} could be achieved. We use artificially created notches in the wire to initiate electromigration and to control the location of the electromigration process. At the position of the notch, electromigration sets in and is observed quasi-continuously by the SEM.

1. Introduction

Electromigration (EM), i.e. the biased motion of atoms induced by current flow (wind force) or by an electric field (direct force) is often responsible for the failure of integrated circuits [1–3]. The wind force is caused by the scattering of travelling electrons on loosely bound atoms and leads to a mass transport in the direction of the electron flow (from cathode to anode). In contrast, the origin of the direct force lies in the electric field that acts on atoms that are not completely shielded by electrons. The direct force leads to a mass flow in a direction opposite (from anode to cathode) that which is observed under the influence of the wind force [4]. Accordingly, in metallic wires the wind force preliminary causes a damage (voids) at the cathode side and hillocks at the anode side, whereas the direct force preferentially creates voids on the anode side and hillocks on the cathode side [5]. The combination of the two forces is usually expressed in terms of the effective charge of the system that describes which of the two forces will dominate the EM behaviour. It has been intensively studied and it is well known that EM processes in polycrystalline Ag samples are dominated by the wind force [1]. Grain boundary diffusion is widely accepted as the dominating mechanism for the transport of atoms due to the wind force. Moreover, it has been shown that the microstructure of metallic wires determines the shape of the voids, their nucleation sites, and how they develop in time [6].

Single-crystalline wires, however, have hardly been investigated [7, 8]. Recently, we found that for single-crystalline Ag nanowires, grown by self-organization of Ag on Si-substrates [9], the direct force seems to be larger than the wind force, since the mass transport occurs opposite to the electron flow [10]. This surprising result suggests that surface diffusion plays the dominating role for EM processes in single-crystalline wires rather than grain boundary diffusion, as the only difference between single-crystalline and polycrystalline wires is the presence of grain boundaries. However, surfaces might be affected by the preparation and in particular by the contacting of the wire. Accordingly, to verify the belief that surface diffusion plays an important role during EM, measurements in an atomically clean environment, i.e. under UHV conditions, are required.

In the present work, we demonstrate that EM studies can indeed be performed on single-crystalline Ag wires under

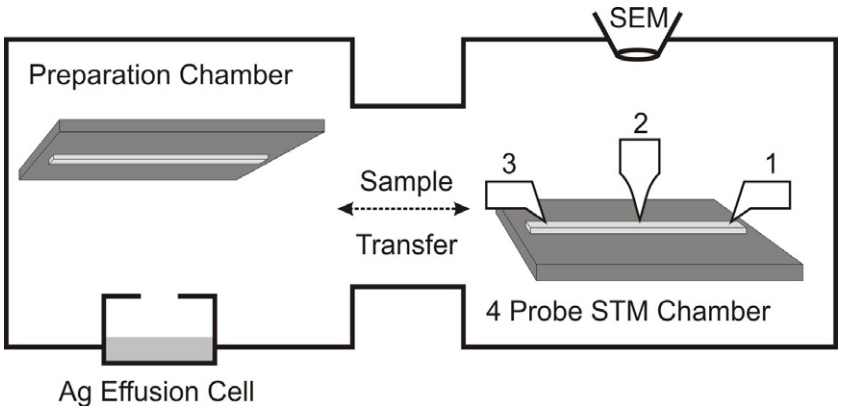

Figure 1. Sketch of the experimental setup. Left: in the UHV preparation chamber, single-crystalline Ag wires are grown on a 4° vicinal Si(001) surface. Right: the EM experiments were performed in a commercial four-probe STM with attached SEM.

UHV conditions, by growing, contacting, and stressing the Ag wire within the same system, without ever exposing the wire to ambient conditions.

2. Experimental details

The experiments were performed in a commercial four-probe STM setup (Omicron Nanoprobe) with an attached UHV preparation chamber for *in situ* preparation and transfer of the samples between the preparation chamber and the STM. Figure 1 shows a schematic drawing of the experimental arrangement. Ag wires were grown *in situ* in the preparation chamber on 4° vicinal Si(001) surfaces, following instructions from the literature [9, 11]. The 4° vicinal Si(001) substrate is transferred into the UHV system, degassed at 600 °C for several hours, and the native protective oxide is removed prior to the Ag deposition by repeated flash annealing of the sample to 1250 °C. The resulting double stepped vicinal Si(001) surface [12] is kept at ∼650 °C during deposition of Ag from a home built effusion cell [13]. Quasi-one-dimensional single-crystalline Ag wires are formed having a typical width and height of a few hundred nanometre. We have been able to grow them to a length of more than 50 μm.

After preparation, the substrate with the Ag wires is transferred into the four-probe STM chamber (Nanoprobe). The Nanoprobe system allows contacting of a single Ag nanowire with two of the STM tips to apply a constant voltage for electrical stressing of the wires with high current densities. To control the current induced modification of the single-crystalline Ag nanowires, a third STM tip is used that provides STM images as well as potentiometry data along the wire axis. In addition to the STM, the system is equipped with an electrostatic scanning electron microscope (Staib SEM) that is used to observe changes of the wire morphology during electrical stressing and provides assistance in placing the contact tips.

Some details of the contacting procedure require further discussion. Once the sample is located inside the nanoprobe, two of the four possible tips (tips '1' and '3' in figure 1) are used for contacting the wire. These two tips are made of Au, i.e. they are soft enough to only cause little damage to the Ag wire while a solid ohmic contact with the wire is established. The tips are approached while observing with the SEM until the tips and their shadows touch (coarse approach). Each tip is then carefully lowered using the z-piezo of that particular tip, until an electrical contact is established (fine approach). This procedure allows placing of the two contact tips at the desired positions, with great accuracy, and little damage to the nanowire.

The third tip, labelled 2 in figure 1, is a standard etched W tip used for STM imaging and potentiometry. After contacting of the wire with tips 1 and 3, we used tip 2 to determine the resistance of the wire and to characterize the quality of the contacts: a constant current is passed through the wire, between contacts 1 and 3. The voltage drop along the wire is then measured with the third tip by adjusting the potential of tip 2, until the average tunnelling current vanishes. The potential at the tip is then equal to the local potential at the surface (bridge balancing). Such non-contact determination of the surface potential at different locations along the wire ensures that the surface of the wire is not modified or damaged during the measurement, which is a crucial requisite for the subsequent EM measurement.

In addition to these electrical measurements, the third tip can also be used for regular STM imaging to determine the shape of the wire, and—complemented by the electrical measurements—allows us to calculate the current density and the specific resistivity of the wire. The fourth tip is also made from W, similar to the third tip, but it is used for structural modifications of the Ag nanowire as will be discussed below.

3. Results and discussion

Figures 2(a)–(f) show a sequence of SEM images taken in between potentiometry measurements for a 19 μm long single crystal Ag nanowire. The six panels at the top of figure 2 show different positions of tip 2 at which the local potential was determined. The potential as a function of the position of tip 2 between tip 1 and tip 3 is plotted (squares) in the bottom of figure 2. Clearly, the wire has an ohmic characteristic. From the slope of the linear fit in figure 2 (solid line) and from the applied total current of 20.3 mA we can determine a

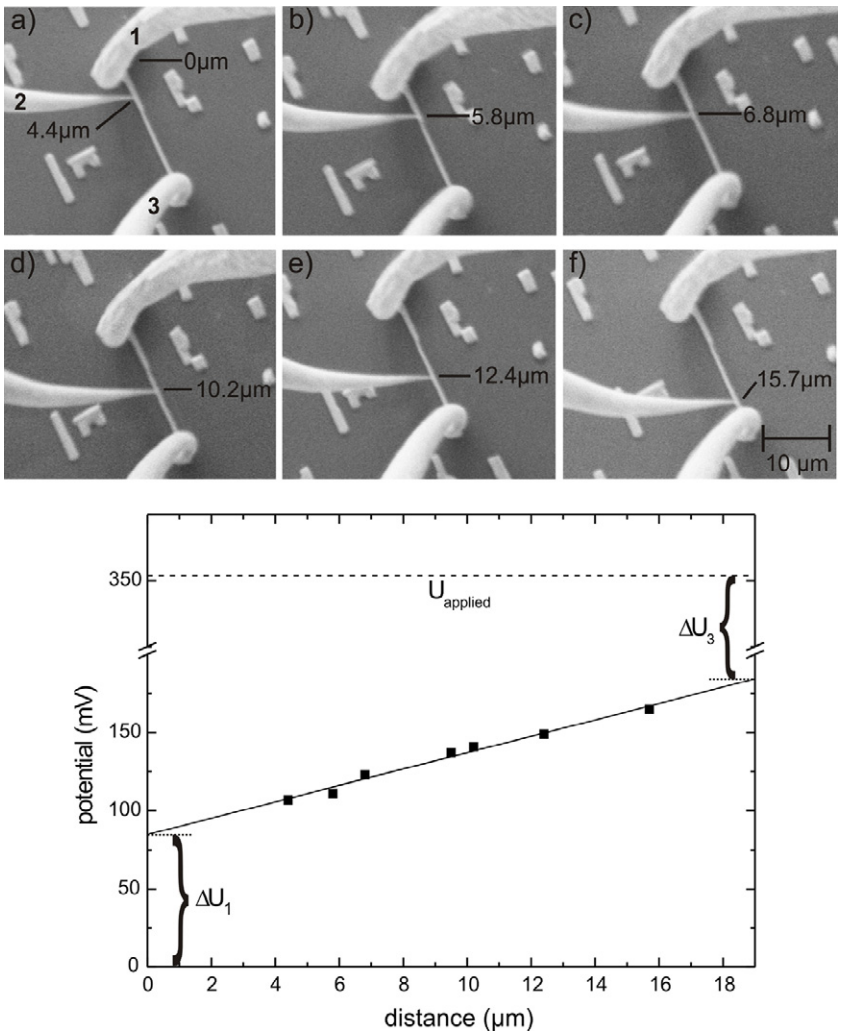

Figure 2. Potentiometry measurements of the Ag nanowire. Top: SEM images of an Ag wire, contacted with Au tips 1 and 3, with the potentiometry tip 2 placed in different locations. Bottom: surface potential along the wire. The intercepts ΔU_1 on the left and ΔU_3 on the right ordinate reflect the contact potential drop of the two contacts, respectively.

resistance per length of the wire of $\mathrm{d}R/\mathrm{d}l = 2.58 \times 10^5\ \Omega\ \mathrm{m}^{-1}$. By extrapolating the linear fit to the positions of the tips, the voltage drop over the part of the wire between the tips, as well as the offset at the contacts, ΔU_1 and ΔU_3, can be determined.

The determination of the resistivity of the wire and the current density requires an accurate knowledge of the shape of the wire. Figure 3(a) shows a topographic STM image, recorded with tip 2, and figure 3(b) shows the wires' cross section at the position marked in panel (a). Integration over the cross section yields a surface area of $A_{\mathrm{wire}} = 0.06 \pm 0.006\ \mu\mathrm{m}^2$ which, considering the measured resistance per length given above, translates into a resistivity of $\rho_{\mathrm{wire}} = 1.55 \pm 0.15\ \mu\Omega$ cm. This value is comparable to the known resistivity of bulk Ag material that is listed as $\rho_{\mathrm{Ag}} = 1.59\ \mu\Omega$ cm at room temperature [14], supporting the high purity and crystallinity of the present Ag wires, grown under UHV conditions.

In determining ρ_{wire}, we limited the current density in the wire to about 3.5×10^6 A cm^{-2} with the intention not to damage the wire during the potentiometry measurements. Thus it is not surprising that we did not observe EM processes under these conditions at all. An increase of the current density up to 10^7 A cm^{-2}, however, was not successful either in causing EM on the visible part of the wire. Instead, the contact tips started moving around and were ultimately ripped off the wire. Considering all resistors involved in the experiment, this is not surprising, since the contact resistances and the resistance of the wire are comparable. Hence, the dissipated power is in the same order of magnitude for the wire and for the contacts. The power density, however, is much higher for the contact region, since the dimensions of the contacts are much smaller than the length of the wire. While the heat can be transferred rather well from the wire to the substrate, this works less well for the contacts. Not unexpectedly, we found that with our simple push-down contacts EM processes in the region between the contacting tips could not be observed, while obviously massive changes of the contact geometry were happening. Rather than attempting to reduce the contact resistance, we chose to simply introduce a notch into the wire. To initiate EM in an area that is accessible to the SEM and that is not hidden under the contacts, we used the fourth STM tip to lightly scratch the wire. While

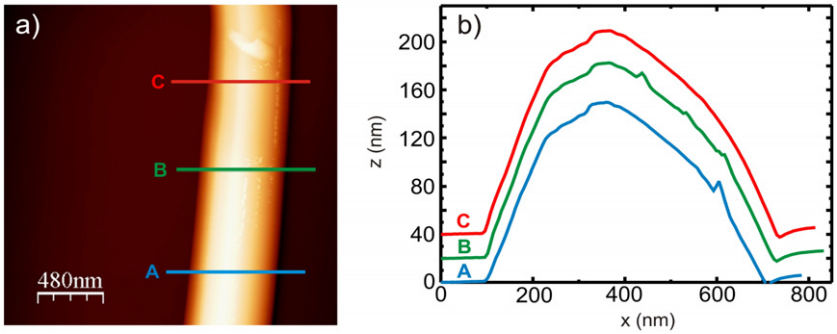

Figure 3. Cross section of a self-organized Ag nanowire. (a) STM image of the wire, (b) three line profiles at the different positions of the wire marked in (a), reflecting the high uniformity of the wire's cross section. The lines B and C are offset by 20 and 40 nm.
(This figure is in colour only in the electronic version)

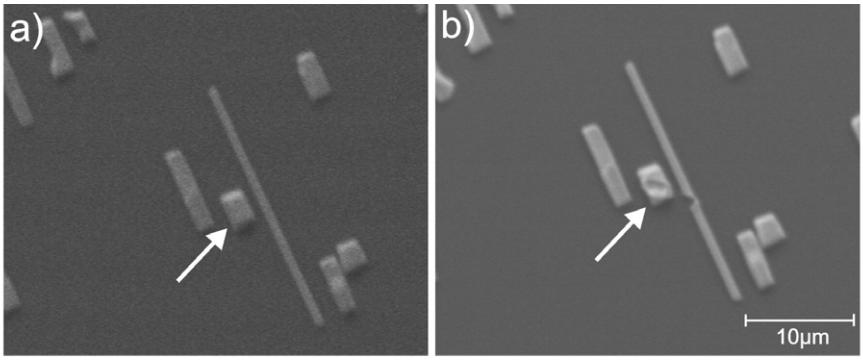

Figure 4. SEM images of an Ag nanowire (a) before and (b) after modification of the wire shape. During modification, the fourth STM tip was lowered and then gently moved to the right to scratch into the wire. Note that the island marked by the arrow was also modified during the scratching procedure.

monitoring with the SEM, we positioned the fourth tip over an area next to the wire, then lowered the tip until an electrical contact with the surface was established. Afterwards, the tip was carefully moved sideways to modify the wire as gently and in as controlled a way as possible.

Figure 4 shows SEM images of an Ag nanowire before and after such modification with the STM tip. Panel (a) shows the intact wire, surrounded by some distinct marker islands. Panel (b) shows the same marker islands surrounding a modified wire that exhibits an area of reduced width in the middle between the contacts (note that the island marked by the arrow in the two panels was also damaged during the scratching). After this reduction of the wires' cross section and contacting of the wire by the procedure as described above, initially a current of $I = 30$ mA was applied to the wire. This current corresponds to a current density in the non-damaged areas of the wire of about 10^7 A cm^{-2}. However, the current density is significantly higher in the narrow region that was created by the scratching. Under these conditions, typical signatures of the EM behaviour of Ag nanowires could be observed [5]. With the SEM it was possible to record a movie of the EM process at a frame rate of three frames/second. Figure 5 shows still images from the movie summarizing the observations.

From the enlarged panel in figure 5(a), one can estimate that by scratching the nanowire, the width of the nanowire is reduced by a factor of ≈3 at the position of the notch. Simultaneously, the resistance is enhanced.

Panels (b)–(d) of figure 5 show SEM images of the scratched Ag nanowire during electrical stressing at 60 s, 90 s (81 mA), and 120 s (110 mA). The arrow in figure 5(b) indicates the direction of the electron flow, 'A' and 'C' denote the anode and cathode side of the wire. The width of the nanowire in the region between the notch and the anode side of the wire is drastically decreased (panel b), compared to the initial width of the wire as displayed in panel (a). The decrease occurs abruptly within less than 1 s, i.e. it was not possible to resolve the thinning of the wire in detail. The trend continues in panels (c) and (d), where at a current of 81 mA (c) and 110 mA (d) the narrow part of the wire extends towards the cathode side of the wire. Such behaviour was also observed for single-crystalline Ag nanowires, contacted and measured *ex situ* [5], and has been explained by EM processes that are dominated by the direct force, rather than the wind force. Such interpretation implies that the mass flow is opposite to the electron flow, i.e. material is transported from the anode side to the cathode side of the wire. Although we find that during stressing of the Ag nanowire the material on the anode side continuously decreases, we do not observe any increase of material on the cathode side in the upper panels of figure 5. Thus, we could not detect in which direction the mass flow proceeded, since material could have been transported to

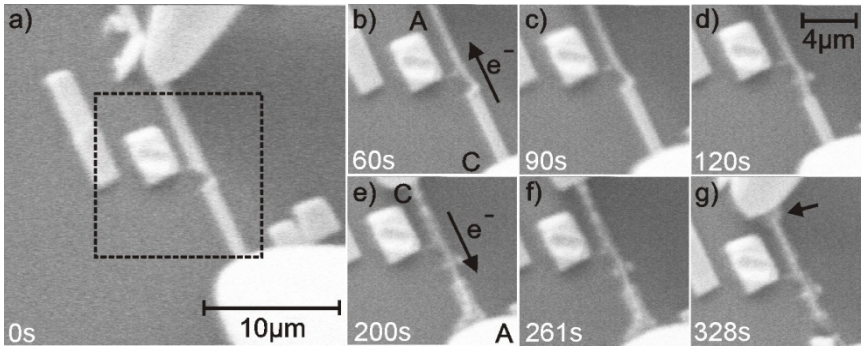

Figure 5. Still images recorded with the SEM during an EM experiment on a scratched wire. (a) Initial configuration. Panels (b)–(g) show only an area of the size of the dashed box in panel (a). (b)–(e) Still images after 60, 90, and 120 s of electrical stressing at a current of 81 mA ((b) and (c)) and 110 mA (d), with the electron flow from the lower right to the upper left. (e)–(g) Still images after 200, 261, and 328 s of electrical stressing at a current of 80 mA, with the electron flow from the upper left to the lower right. 'A' and 'C' mark the anode and cathode side of the wire in panels (b) and (e), respectively.

either one of the areas below the anode tip or the cathode tip. Considering the temperature profile of the Ag wire, however, provides further support for our claim of direct force EM. Obviously, the highest temperature in the wire is located near the notch, resulting in enhanced mass transport in its vicinity. If the mass transport is opposite to the electron flow (direct force), material is moved from the anode to the cathode side of the wire across the notch. Such migration shifts the peak of the temperature distribution towards the anode. Ultimately, this results in a progressive thinning of the wire at the anode side of the notch—the result of which is visible in panel (b). If the wind force was responsible for the observed EM, the argument would have to be reversed and would predict progressive thinning at the cathode side, which in turn is not compatible with the observation.

Figures 5(e)–(g) show SEM images of the same Ag nanowire during electrical stressing after reversal of the current direction and adjusting the total current to 80 mA. Here we observe that the wire exhibits irregular structures, indicative of melting processes that are caused by the high current densities and the corresponding temperature increase [15]. However, one still finds that material is removed from the anode side until the wire breaks down (figure 5(g)). A closer inspection of figures 5(f) and (g) even shows that the thickness of the nanowire increases on the cathode side of the wire, exhibited by the smoother topography of the wire. Furthermore, a hillock can be detected directly next to the cathode tip (see the arrow in panel (g)).

Our observation suggests that the Ag was transported in a direction opposite to the current direction, which has also been observed for single-crystalline Ag wires in earlier *ex situ* EM experiments [10]. Accordingly, the direct force seems to be responsible for the EM processes in the single-crystalline Ag nanowires, instead of the wind force; independently of whether the EM experiments are performed under UHV conditions or not. This is surprising, since one would expect that EM, if based on surface diffusion processes, should be strongly affected by surface modifications that are unavoidable during the typical *ex situ* electron beam lithography contacting.

4. Conclusions

Our experimental study constitutes the first all-UHV, all-*in situ* EM study of self-assembled Ag nanowires to date. Growing Ag nanowires inside a UHV chamber and controlling the result by SEM, followed by contacting of the wires by a four-probe STM is a very controlled way to prepare test structures for *in situ* EM experiments. Such well-defined experimental conditions provide a controlled and reliable experiment, since possible surface contaminations are simply excluded and do not have to be considered during interpretation of the results. We note that in contrast to the findings of Shi *et al* [16], substrate contributions are not taken into account for the EM observations since the current is driven directly through the nanowire. In addition we expect the diffusion activation energy to be much smaller on top of the nanowire than at the nanowire/substrate interface.

Our EM results, shown in figure 5 not only demonstrate that we could indeed perform such a controlled experiment, but the experimental data also gives a hint in which direction the mass transport occurs. In agreement with earlier observations [10], we find the direct force to be the effective mechanism for EM in the single-crystalline Ag nanowires. Apparently, the direct force overcompensates the wind force in our case. We believe that enhanced surface diffusion—compared to the preferred grain boundary diffusion in polycrystalline wires—is the reason for the reversal of the EM direction. Further *in situ* STM and potentiometry measurements under UHV conditions are in progress to clarify the validity of this proposition.

The present experiments under UHV conditions provide the opportunity for studying the impact of surface modifications on EM processes. Such experiments will ultimately provide insight into why the direct force seems to be the dominating EM process in the single-crystalline wires.

Acknowledgment

The authors acknowledge financial support from the Deutsche Forschungsgemeinschaft under programme 'SFB616: Energy Dissipation at Surfaces'.

References

[1] Ho P 1989 *Rep. Prog. Phys.* **52** 301–48
[2] Pierce D G 1997 *Microelectron. Reliab.* **37** 1053–72
[3] Tu K N 2003 *J. Appl. Phys.* **94** 5451
[4] Sorbello R S 1988 *Solid State Physics* vol 51 (New York: Academic) p 159
[5] Stahlmecke B, Chelaru L, Meyer zu Heringdorf F-J and Dumpich G 2006 *AIP Conf. Proc.* **817** 65–70
[6] Arzt E, Kraft O, Nix W D and Sanchez J E 1994 *J. Appl. Phys.* **76** 1563
[7] Shingubara S, Nakasaki Y and Kaneko H 1991 *Appl. Phys. Lett.* **58** 42
[8] Yoo Y-C and Thompson C V 1997 *J. Appl. Phys.* **81** 6062
[9] Roos K R, Roos K L, Horn-von Hoegen M and Meyer zu Heringdorf F-J 2005 *J. Phys.: Condens. Matter* **17** 1407
[10] Stahlmecke B, Meyer zu Heringdorf F-J, Chelaru L, Horn-von Hoegen M, Dumpich G and Roos K R 2006 *Appl. Phys. Lett.* **88** 053122
[11] Tersoff J and Tromp R M 1993 *Phys. Rev. Lett.* **70** 2782
[12] Fölsch S, Winau D, Meyer G, Rieder K H, Horn-von Hoegen M, Schmidt T and Henzler M 1995 *Appl. Phys. Lett.* **67** 2185
[13] Kury P, Hild R, Thien D, Günter H, Meyer zu Heringdorf F-J and Horn-von Hoegen M 2005 *Rev. Sci. Instrum.* **76** 083906
[14] Giancoli D C 2006 *Physik* (Munich: Pearson Studium)
[15] Stahlmecke B and Dumpich G 2007 *J. Phys.: Condens. Matter* **19** 046210
[16] Shi F X, Yao W Q, Cao L L and Dong Y H 1997 *J. Mater. Sci. Lett.* **16** 1205–7